Calorimetric Features of High-Enthalpy Amorphous Solids and Glass-Softening Temperature of Water

G. P. Johari*

Department of Materials Science and Engineering, McMaster University, Hamilton, Ontario L8S 4L7, Canada

Received: January 8, 2003; In Final Form: June 3, 2003

In the differential scanning calorimetry (DSC) scans of the annealed states of vapor-deposited, hyperquenched, and crystal-amorphized solids, the glass-softening or T_g endotherm is interrupted by the crystallization exotherm, thus making the T_g endotherm appear like a rounded peak. This apparent peak is occasionally misidentified as a sub-T_g peak, which appears in the $0.7T_g$ to $0.8T_g$ range in the DSC scan of glasses preannealed at a specific temperature, T_{ann}. To help prevent such misidentification, we provide four criteria for distinguishing the apparent peak of the T_g endotherm from a sub-T_g peak: (i) Crystallization occurs in the T_g endotherm range or at T just above it, and *not* in the sub-T_g peak range. (ii) The T_g endotherm onset occurs at $T > T_{ann}$, but the sub-T_g peak onset occurs at T_{ann}. (iii) *Unannealed* glasses show a T_g endotherm; *only preannealed* glasses show the sub-T_g peak, and the height of the sub-T_g peak and its area vary when T_{ann} and the annealing time are varied. (iv) Slope of the DSC scan may decrease, become zero or become negative prior to the onset of the T_g endotherm, but it does not decrease and remains positive prior to the onset of sub-T_g peak. The annealed state of hyperquenched glassy water is known to crystallize in the 142−150 K range of its endotherm, the onset temperature of the endotherm is higher than T_{ann}, its *unannealed state* shows the T_g endotherm, and the slope of the scan prior to the onset temperature is *not* always positive. These observations remove the basis for a recent conjecture that the T_g of water is between 165 and 180 K, and is unobservable. Available calorimetric data on vapor-deposited, hyperquenched, and mechanically amorphized solids have shown a T_g endotherm partially superposed by the crystallization exotherm, but T_g itself does not change. It is proposed that intermediate states formed during the occurrence of disorder−order transitions in solids and in proteins can be studied in the time domain by using their hyperquenched glassy and mechanically amorphized states.

1. Introduction

Most liquids can be vitrified by supercooling to a temperature at which their viscosity exceeds 10^{13} P. But low molecular weight hydrocarbons, molten metals, and water crystallize rapidly on supercooling and cannot be vitrified by the usual cooling methods. Their amorphous state is obtained by depositing vapors on a cold substrate, hyperquenching the liquid, or mechanically deforming their crystals.[1−5] The relatively high frozen-in enthalpy and entropy of this amorphous state are released on heating, and the differential scanning calorimetry (DSC) heating scan shows a broad exotherm. This exotherm overwhelms the characteristic endotherm (or heat capacity rise) due to glass softening, and this characteristic feature is not observed. When such an amorphous solid is isothermally annealed or else heated at a controlled rate and structural relaxation occurs, it loses most of its extra frozen-in enthalpy,[5] and the DSC heating scan of the now preannealed state shows the onset of a sigmoid-shaped endotherm as the mechanically rigid state becomes a viscous liquid. Immediately after the onset of this endotherm, the viscous liquid crystallizes rapidly and a strong exotherm appears.[4−17] When the glass-softening endotherm is weak or is spread out in temperature or both, its proximity to a strong exotherm produces a rounded asymmetric peak with a steep (and negative) high-temperature slope.[4−17] The onset temperature of the endotherm is taken as T_g, the glass-softening temperature, at which the liquid's viscosity is in the range $10^{12}−10^{13}$ P. Such an endotherm has yielded the T_g of water as 136 K.[8−11] (To maintain that no real structural transition occurs at T_g and that a glass becomes progressively softer and, ultimately, a viscous liquid in the T_g range, we use the term "glass-softening" instead of the term "glass-transition" but maintain the T_g notation.)

As early as in 1978, Drijver et al.[18] had reported that the DSC scan of the preannealed state of a hyperquenched glassy metal alloy shows two endothermic peaks instead of only one that is observed for normally cooled glasses. The first peak, with onset T equal to the annealing temperature, T_{ann}, was small and broad, and the glassy state was maintained over the range of this peak. The second peak, with onset T much higher than T_{ann}, was relatively sharp, and its shape was a consequence of the T_g endotherm being interrupted by crystallization of the viscous liquid. Chen and co-workers[19−28] have thoroughly studied the characteristics of this first (or additional) peak in the DSC scans of a variety of hyperquenched glassy metal alloys and other glasses. They called the first peak the "sub-T_g peak" and provided a theory based on the distribution of structural relaxation times for its appearance.[19,26] (This peak has recently been called by two other names, "annealing pre-peak" and "shadow-T_g peak"[29] without reference to the earlier studies,[18−28] but we retain the original and frequently used term "sub-T_g peak" after those who discovered it, showed it to be a characteristic feature of glasses, and provided its interpretation in terms of the structure of a glass.[19−28]) The sub-T_g peak appears only for a glass preannealed for a certain time at a certain temperature,

* To whom correspondence should be addressed. Electronic mail: joharig@mcmaster.ca.

10.1021/jp030009y CCC: $25.00
Published on Web 07/18/2003

and the temperature range of this peak varies with the annealing conditions.[18−28] We point out that the sub-T_g peak has been observed also in the DSC scan of a preannealed B_2O_3 glass, which had been made by cooling the melt at an 80 K/min rate.[22] This means that hyperquenching is *not* a requirement for its appearance and that both its appearance and feature depend on the preannealing conditions. Also, the sub-T_g peak is found to be a manifestation of the so-called memory effect arising from the distribution of relaxation times in the glass structure.[19−28]

The above-described apparent peak of the T_g endotherm has been occasionally mistaken for a sub-T_g peak, thus leading one to infer that a material's true T_g is 25%−30% higher than the T_g deduced from the observed endotherm and that the true T_g endotherm was not observed because the *glass crystallized* at a temperature *far below* its true T_g. If valid, such an inference has consequences not only for our understanding of the properties of glasses but also for their technical use, because it would then require that we reinterpret the changes observed in the vapor pressure, heat capacity, dielectric and mechanical relaxations, electrical conduction, viscosity, self-diffusivity, phonons, etc. of glasses at both high and low temperatures, rewrite specifications for their shaping and stress-removal procedures, and respecify the useful life of the magnetic, electrical, and mechanical devices made from such solids. Obviously, there is a need for criteria useful for distinguishing the apparent peak of a T_g endotherm from a sub-T_g peak. With the growing interest in amorphous state, this need has been increasingly felt.

Upon the basis of our understanding of structural relaxation and crystallization phenomena and by analyzing the available experimental studies here, we deduce four main criteria for distinguishing the apparent peak of a T_g endotherm from a sub-T_g peak. We then use these criteria to characterize the observed DSC features of the preannealed states of hyperquenched glassy water (HGW) and amorphous solid water (ASW). We find that their DSC features fulfill the requirements for the T_g endotherm and not those for a sub-T_g peak. This seems to remove the basis for the suggestion that the T_g of water is in the 165−180 K range and is unobservable.[29] Where necessary, we also provide background information on high-enthalpy amorphous solids and their glass-softening and crystallization features. We also provide a list of high-enthalpy glasses, of which the DSC features are useful for understanding crystallization of viscous liquids and which are qualitatively similar to those of HGW and ASW. Finally, we mention the use of quenched glasses in understanding the nature of phase transformations in solids and in proteins.

2. High-Enthalpy Amorphous Solids and Their Thermodynamics

As mentioned earlier here, when usual supercooling fails to vitrify a liquid, other techniques are used for producing its amorphous solid (for details, see flowcharts in refs 1 and 2). These techniques are[1−5,30−45] (i) hyperquenching (cooling at a 10^5−10^6 K/s rate) the liquid,[8,19−26] (ii) shock-compressing the liquid and then cooling, (iii) rapidly precipitating from a solution, (iv) slowly depositing vapors on a cold substrate, (v) irradiating crystals by neutrons, α-particles, electron beam, and ultraviolet rays,[30] (vi) rapidly dehydrating a crystal,[1,2,30] (vii) collapsing crystals under a uniaxial pressure,[31−33] and (viii) randomly deforming crystals by techniques of ball milling.[34−45] Physical properties of the amorphous solid produced by these methods differ from those of a usual glass. Moreover, when such solids contain micrometer-size or distorted crystals or both, their physical properties further vary with the amount of the crystal phase and its morphology. It is to be noted that properties of covalently bonded and hydrogen-bonded network structure amorphous solids also depend on the topology of the network formed and on the populations of the unbonded atoms or molecules in it,[46,47] thus giving rise to what is known as polyamorphism. In 1970, Roy[1] had described the polyamorphism of SiO_2.

Structural relaxation of these high-enthalpy amorphous solids has been found to occur at a rate several orders of magnitude faster than that of ordinary glasses with release of heat as large as 1−2.8 kJ/mol before their equilibrium state is approached.[5,30,42,44,45,48] This heat appears as a local but broad exothermic minimum in the DSC scan and as a spontaneous temperature rise in an adiabatic calorimetry experiment. The structural relaxation exotherm of such solids begins at a much lower T than that for a low-enthalpy glass (see ref 49 for details), which means that atomic or molecular self-diffusion in high-enthalpy amorphous solids is faster than that in the low-enthalpy glasses. The broad and pronounced exotherm often masks the onset region of the T_g endotherm and, for certain annealing or heating conditions or both, the structural relaxation exotherm persists at high enough temperatures to overlap the usual range of the T_g endotherm.[49] In most such cases, the viscous liquid state achieved at $T > T_g$ crystallizes rapidly either within the range of the sigmoid-shaped T_g endotherm or immediately after completion of the endotherm, depending upon the heating rate. The resulting strong exotherm masks the high-temperature part of the sigmoid-shaped T_g endotherm in a DSC scan. This rapid crystallization also prevents one from measuring the viscosity and other properties of its equilibrium liquid. Examples of materials that crystallize rapidly soon after the onset of their T_g endotherm are vapor-deposited CCl_4 (see Table 1 in ref 43) and a variety of hydrocarbons,[3−5] hyperquenched metal alloys (atomic glasses of high fictive temperatures),[17−20,23−26,50,51] ASW,[13] HGW,[8,9,52] mechanically amorphized solid 1,3,5-tri-α-naphthylbenzene (a molecular glass),[44,45] etc. When such amorphous solids already contain crystal nuclei or microcrystals or both on their surface or in their bulk, they crystallize even more rapidly on heating, as, for example, some glassy metal alloys,[15] and ASW,[9] HGW,[8,9,52] and mechanically amorphized solids.[41−45]

It should be noted that several glasses have been found to crystallize also at T below their T_g, but only after having been kept for a long period at that T. Among these are a few Ni-based, hyperquenched metal alloy glasses,[50,51] which crystallize *incongruently* and relatively slowly over a period of several hours to several days when kept at temperatures slightly *below* T_g. Our scrutiny of the calorimetric data on these glasses has shown that the ratio of the crystallization temperature of their unannealed state to T_g is 0.99 for $Ni_{75}P_{16}B_6Al_3$,[50] 0.91 for $Fe_{40}Ni_{40}B_{20}$,[51] and 0.97 for $Fe_{40}Ni_{40}P_{14}B_6$.[51] Therefore, even incongruent crystallization of these glasses occurs only at $T > 0.91T_g$ and only when they are annealed over a period 10^3−10^4-times the mathematically equivalent period of the isothermal step of a DSC scan. Whether these glasses were free from microcrystals is not certain, but even in these cases of slow crystallization, T_g is at most 10% higher than the incongruent crystallization temperature. Because T_g does not correspond strictly to isoviscosity conditions and depends on the heating rate used, its value is not unique, and therefore, it is not surprising that some glasses can crystallize at T slightly below their apparent T_g over a period of hours to days.

To reveal the T_g endotherm, the frozen-in enthalpy of such solids has to be released slowly at a low temperature. This has

been done by (i) heating the solid at a rate of 1−2 K/min up to a suitable temperature, (ii) thermal cycling the solid within a narrow temperature range, or (iii) annealing it isothermally at a suitably low temperature.[8−12] After the frozen-in enthalpy of a sample has been thus substantially decreased, its DSC heating scan obtained at a 10−40 K/min rate has shown its characteristic T_g endotherm. This anneal-and-scan procedure had been developed and successfully used for revealing the T_g endotherm of water,[8−12] aqueous solutions,[53,54] and a variety of rapidly crystallizing metal alloy glasses.[15]

3. The Apparent Peak of the T_g Endotherm and the sub-T_g Peak in DSC Scans

We mentioned earlier here that the (rounded-peak) shape of a T_g endotherm is an artifact of crystallization occurring soon after an amorphous solid has softened to a viscous liquid and that its temperature range and shape varies with the nature of crystallization kinetics and the amount, the size, and the distribution of crystal nuclei already present in the solid. Therefore, the high-temperature part of the apparent peak of the T_g endotherm is often irreproducible from one sample to another and depends on the sample preparation conditions [see ref 49 for details]. As an example of such an apparent peak of the T_g endotherm, we show in Figure 1A two DSC scans for a bulk-cooled $Zr_{41}Ti_{14}Cu_{12.5}Ni_{10}Be_{22.5}$ glass measured during heating at a 5 K/min rate in one case and at a 10 K/min rate in the second case (data taken from Figure 3 in ref 17). We also show in Figure 1B a DSC scan for a bulk-cooled $Zr_{41}Ti_{14}Cu_{12.5}Ni_5Fe_5Be_{22.5}$ glass measured during heating at a 10 K/min rate (taken from the DSC scan labeled $x = 5$ in Figure 1 of ref 17) with T_g of the two glasses indicated by arrows. These glasses had been produced by quenching the molten alloy in water. The solids thus obtained were not annealed deliberately, and the featureless part of their DSC scan at low temperatures had been excluded from the published scans.[17] Note that the negative slope of the scan obtained for heating at 5 K/min and nearly zero slope obtained for heating at 10 K/min heating rate are a consequence of the enthalpy relaxation of the unannealed glass. This is a common observation described in a number of studies.[49,55,56]

The sub-T_g peak arises from relaxation effects during the heating of a preannealed sample, and the sample deforms in the apparent peak of the T_g endotherm, but it *does not* deform in the sub-T_g peak range. Chen and co-workers[19,22,26] have provided extensive data on this subject, constructed the enthalpy plots from the DSC scans, and described the underlying relaxation effects in terms of a distribution of relaxation times. The sub-T_g peak also has been observed for preannealed B_2O_3 glass[22] that had *not* been hyperquenched; it had been obtained by cooling the melt at an 80 K/min rate. This shows that the sub-T_g peak is *not* a property of the preannealed hyperquenched state.

Therefore, when a glass preannealed at a certain T_{ann} is studied by DSC, its heating scan usually shows first a sub-T_g peak and then a deep local minimum. After this minimum, a sigmoid-shaped endothermic rise appears, which is attributed to the glass softening. This rise terminates at a small peak, known as overshoot, and finally the equilibrium liquid state is reached. The overshoot is attributed to the enthalpy recovery. All four features have been observed for B_2O_3 glass,[22] as well as for a variety of metal-alloy glasses of which the viscous liquid had been too slow to crystallize at $T > T_g$. Examples of the latter may be found in Figure 7a of ref 26. In contrast, when the viscous liquid crystallizes rapidly, the T_g endotherm is cut off by a sharp exothermic decrease. In this case, only the sub-T_g peak and the local minimum is observed, as, for example, in the DSC scans of hyperquenched metal-alloy glasses in Figure

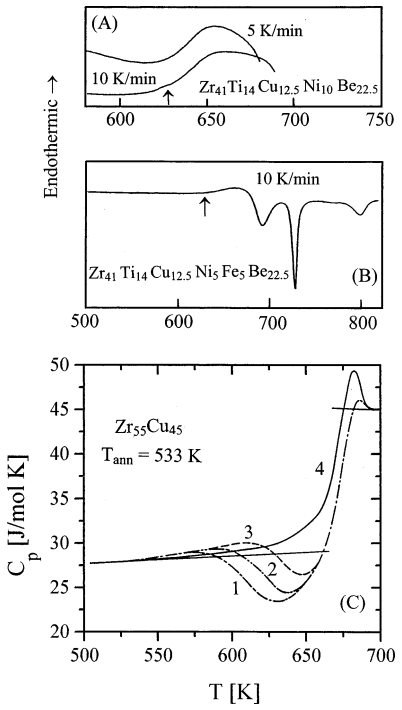

Figure 1. Panel A shows the DSC scans of the quenched $Zr_{41}Ti_{14}Cu_{12.5}Ni_{10}Be_{22.5}$ glass measured at two heating rates, 5 and 10 K/min. Note that the exothermic decrease in (dH/dt) due to crystallization overwhelms the endothermic increase in (dH/dt) due to glass softening and thus produces a rounded peak, which may be mistaken for a sub-T_g peak. The T_g of the metal alloy glass is 626 K, as indicated by the arrow. DSC data are adapted from ref 17 with permission, copyright 1999, American Institute of Physics. The negative slope of the scan obtained for 5 K/min heating and nearly zero slope for 10 K/min heating rates are a consequence of the enthalpy relaxation of the unannealed glass. This is a common observation for unannealed glasses, as discussed in a number of studies.[49,55,56] Panel B shows the DSC scan of the quenched $Zr_{41}Ti_{14}Cu_{12.5}Ni_5Fe_5Be_{22.5}$ glass measured at a 30 K/min heating rate. Note that the exothermic decrease in (dH/dt) due to crystallization overwhelms the endothermic increase in (dH/dt) due to glass softening and thus produces a rounded peak, which may be mistaken for a sub-T_g peak. T_g of the glass is 622 K (indicated by the arrow), and the crystallization onset temperature is 675 K. The DSC scan is adapted from ref 17 with permission, copyright 1999, American Institute of Physics. The nearly zero slope for the 10 K/min heating rate is a consequence of the enthalpy relaxation of the unannealed glass. This is a common observation for unannealed glasses, as discussed in a number of studies.[49,55,56] Panel C shows the DSC scans of the hyperquenched $Zr_{55}Cu_{14.5}$ glass measured at a 40 K/min heating rate. The measured (dH/dt) divided by the heating rate is represented as time- and temperature-dependent C_p. The various C_p curves correspond to different thermal histories, and the straight lines are linear extrapolations from the high- and low-temperature limits of the measurements. Curve 1 is for a sample that had been annealed for 1 h at the annealing temperature, T_{ann}, of 533 K, curve 2 is for that annealed for 3 h at 533 K, and curve 3 is for that annealed for 12 h at 533 K. Curve 4 is for a sample preconditioned to remove most of its excess enthalpy. The T_g as determined from curve 4 is ca. 660 K. Note that the onset temperature of the broad sub-T_g peaks observed for curves 1, 2, and 3 is the same as T_{ann}, that is, 533 K. There is an overshoot in the apparent C_p before the equilibrium liquid state is reached at T near 700 K. The crystallization temperature is slightly higher than 700 K. The scans are adapted from ref 26 with permission, copyright 1985, Chapman and Hall. The sub-T_g peak and its shift with increase in the annealing time is a manifestation of the memory effect and requires consideration in terms of a distribution of relaxation times and a change in the structure. Note also the crossing-over of curve 4 by curves 1, 2, and 3 at different temperatures.

1 (curve 2), Figure 2 (curves 3 and 4), and Figure 3 (curves 2, 3, and 4) in ref 15.

To illustrate the difference between a sub-T_g peak and a T_g endotherm, four DSC scans from Figure 8a in ref 26, which had been obtained by heating $Zr_{55}Cu_{45}$ glass at a 40 K/min rate, are provided here in Figure 1C. The data had been presented[26] as time- and temperature-dependent heat capacity, C_p, which is directly proportional to dH/dt, that is, the DSC scan signal. The $Zr_{55}Cu_{45}$ glass was made by melt spinning, a procedure used for hyperquenching ductile materials. Curves 1, 2, and 3 are for hyperquenched samples that had been preannealed for 1, 3, and 12 h, respectively, all at T_{ann} of 533 K, and these show a true sub-T_g peak of which the broad maximum is at ca. 572, 589, and 610 K, respectively. Clearly, the sub-T_g peak is far more spread out than the T_g endotherm, and in all cases, the sub-T_g peak begins at T_{ann} of 533 K. Curve 4 in Figure 1C is the "standard scan" for a "preconditioned" sample, that is, one that had been heated to $T > T_g$, equilibrated, cooled at a relatively slow rate, and reheated without annealing. Comparison of the T_g endotherms of the two curves (one in Figure 1A and the other in Figure 1B) against the sub-T_g peak of curves 1, 2, and 3 in Figure 1C shows that the two curves in Figure 1A,B have a much steeper slope on the high-temperature side of the peak of the T_g endotherm than curves 1, 2, and 3 in Figure 1C. Because the crystallization exotherm at $T > T_g$ is much steeper than the high-temperature side of a sub-T_g peak, the difference between their steepness alone can be sufficient for distinguishing an apparent peak of the T_g endotherm from a sub-T_g peak. But if, in an unlikely case, one assumes that crystallization also begins on the high-temperature side of a sub-T_g peak, that is, in the rigid state of a glass, and makes the slope steeper, additional criteria are needed for distinguishing a T_g endotherm from a sub-T_g peak.

4. T_g Endotherm Appearing Like a Sub-T_g Peak

It has been mentioned here that the apparent peak of the T_g endotherm observed for a rapidly crystallizing glass resembles a sub-T_g peak. To show a case in which a *known* T_g endotherm appears like a sub-T_g peak, we searched for the DSC studies of a material that had been vitrified by the usual cooling, as well as made amorphous by mechanically deforming its crystals. We found that the amorphous state of 1,3,5-tri-α-naphthylbenzene has been produced by both procedures, and these states have been studied by Tsukushi et al.[45] Mechanically amorphized solid in their study had shown no Bragg peaks in the X-ray diffraction pattern, thus indicating that any crystallites present were highly mechanically deformed or submicrometer in size or both. Its frozen-in high enthalpy was found to rapidly decreased on heating. Yamamuro et al.[44] have measured its DSC scan by heating at 3 K/min, which allowed more time for the rapid enthalpy decrease over a small temperature range. They also studied its glass obtained by slowly cooling its melt. The DSC data taken from their Figure 3 (insert) in ref 44 for both the melt-cooled glass and the mechanically amorphized solid are shown here in Figure 2A. The melt-cooled glass shows a typical sigmoid-shaped T_g endotherm. The mechanically amorphized solid also shows this endotherm, but this endotherm is overwhelmed by the onset of the rapid crystallization exotherm of its viscous liquid (the deep minimum of which is not shown) with the consequence that a rounded peak appears. Because this onset occurs at a temperature far below the maximum of the endotherm, the line intersection method for determining the T_g value becomes less reliable for the mechanically amorphized solid, and therefore, Yamamuro et al.[44] used a half-height method to determine T_g. They reported that T_g for both the melt-cooled glass and mechanically amorphized solid is 345 K.

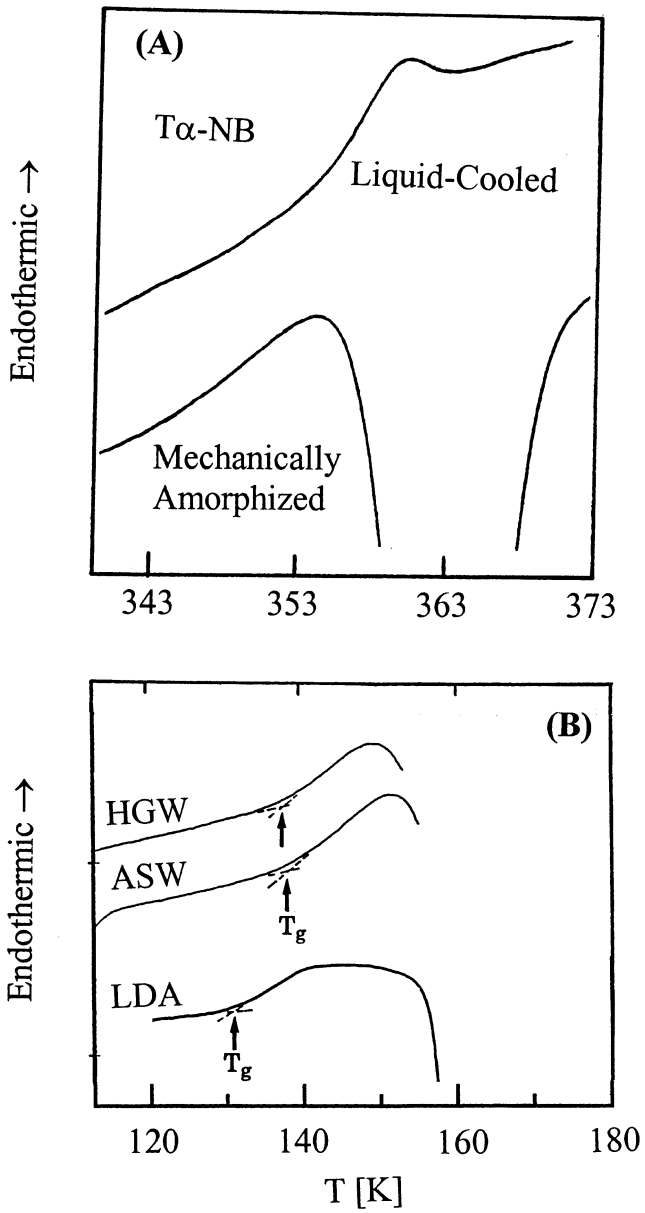

Figure 2. Panel A shows the DSC scans for liquid-cooled and mechanically amorphized 1,3,5-tri-α-naphthylbenzene (T-αNB), as indicated. The heating rate was 3 K/min. The liquid-cooled glassy state shows a slight overshoot before reaching the equilibrium liquid state. Note that the exothermic decrease in (dH/dt) resulting from crystallization overwhelms the endothermic increase in (dH/dt) due to glass softening. This produces a rounded peak, which may be mistaken for a sub-T_g peak. T_g's of the glass and the mechanically amorphized solid were estimated as ca. 345 K. Adapted from ref 44 with permission, copyright 1996, OPA, Amsterdam. Panel B shows the DSC scans of preannealed states of hyperquenched glassy water (HGW), vapor-deposited amorphous solid water (ASW), and the low-density amorph (LDA). The heating rate was 30 K/min. The T_g values have been indicated. Note that the exothermic decrease in (dH/dt) due to crystallization to cubic ice overwhelms the endothermic increase in (dH/dt) due to glass softening and thus produces a rounded peak, which may be mistaken for a sub-T_g peak. The DSC scans are adapted from ref 84 with permission, copyright 2000, Elsevier.

For our purpose we note that (i) the broad peak in the DSC scan of the mechanically amorphized solid does resemble the sub-T_g peak shown in Figure 1C and (ii) the amorphous solids formed by these two methods, with their initially different thermodynamic properties, have similar T_g endotherm onset

features. It should be stressed that the sigmoid-shaped endotherm of 1,3,5-tri-α-naphthylbenzene glass cannot be seen as a sub-T_g peak because the T_g,[57−59] heat capacity,[57] viscosity,[60,61] crystallization kinetics,[62,63] creep recovery[60] and viscoelastic relaxations,[64] and aging effects[59,65] of 1,3,5-tri-α-naphthylbenzene have all been studied in detail. Its viscosity has been found to be ca. 10^{13} P at 345 K, and its T_g is unambiguously known to be 345 K for a 20 K/min heating rate.[59] (Note that these earlier studies had been made on an isomer of 1,3,5-tri-α-naphthylbenzene.[58,59,66])

We conclude that if we were to identify the apparent peak of the T_g endotherm observed for the mechanically amorphized solid 1,3,5-tri-α-naphthylbenzene as its sub-T_g peak, we would deduce incorrectly, as has been done for water in ref 29, that T_g of 1,3,5-tri-α-naphthylbenzene is 20%−30% higher than 345 K, that is, it is 414−449 K. We would also incorrectly deduce that the T_g of 1,3,5-tri-α-naphthylbenzene is unobservable because its *glass* crystallizes at $T > 353$ K, the peak temperature for its mechanically amorphized solid.

5. Criteria for Distinction between a T_g endotherm and a Sub-T_g Peak

First, it should be noted that the apparent peak of the T_g endotherm is an artifact from superposition of the crystallization exotherm on the glass-softening endotherm. In contrast, the sub-T_g peak is entirely a structural relaxation effect. For distinguishing an apparent peak of the T_g endotherm from a sub-T_g peak, we provide the following four main criteria: (1) An amorphous solid produced by methods mentioned in section 2 crystallizes when kept at a temperature within the T_g endotherm range. Such solids have *not* been found to crystallize when kept in the sub-T_g peak range, and even liquids that are most difficult to supercool have been found to remain stable when kept at T within their sub-T_g peak range. Also, when such solids are heated through the T_g endotherm range, the viscosity decreases from ca. 10^{13} to 10^{11} P. But on heating through the sub-T_g peak range, *no* such viscosity decrease occurs. (2) The onset temperature of a T_g endotherm is always higher than T_{ann}. On the contrary, the onset temperature of a sub-T_g peak is found to be the *same as* the preannealing temperature, T_{ann}.[18−28] (3). Both the preannealed and unannealed glasses show a T_g endotherm. But *only* a preannealed glass shows the sub-T_g peak. After the sub-T_g peak, the DSC scan crosses the DSC scan of the normal cooled unannealed glass from above (curves 1, 2, and 3 crossing over curve 4 in Figure 1C here, and Figure 7 in ref 26). The height and area of the peak increase when T_{ann} is kept fixed and the annealing time is increased or when the annealing time is kept fixed and T_{ann} is increased or both. In both cases, the crossover temperature increases. (4) When an *unannealed* glass is heated, its structure relaxes and the heat released decreases the slope of the DSC scan, in some cases even to a negative value, as T increases toward the onset temperature of the T_g endotherm. (The extent of decrease in the slope depends on the ratio of the cooling rate to heating rate. When this ratio is less, the decrease is less and the slope may remain slightly positive or zero, and when this ratio is high, the decrease is large and the slope may even become negative, as is evident from the DSC scans of two glasses shown in Figure 1A,B. More examples of such weakly positive, zero, or negative DSC scan slopes at $T < T_g$ are found in a monograph on glass relaxation[55] and in a number of papers cited in ref 56.) In contrast, the slope of the DSC scan of a preannealed glass remains positive and does not decrease prior to the appearance of the sub-T_g peak because any relaxation of a preannealed glass to a lower energy state on its heating from T_{ann} to the onset temperature of the sub-T_g peak is usually insignificant.[18−28] Thus if the DSC scans of a preannealed, as well as an unannealed, glass were to show different (zero and negative) slopes prior to the onset of the endotherm but similar onset temperatures, the peak observed would be an apparent peak of the T_g endotherm and not a sub-T_g peak.

6. The DSC Endotherm and the T_g of Water of 136 K

We mentioned in section 2 that the anneal-and-scan procedure had been developed[8] for determining T_g of water, which had been vitrified by hyperquenching its micrometer-sized droplets[67,68] or else made amorphous by depositing vapors on a substrate kept at 77 K. In the DSC scan of preannealed glassy water, the T_g endotherm was found to be superposed by its crystallization exotherm, and this had caused the sigmoid-shaped endotherm to appear as a rounded peak with sharply downward slope on the high-temperature side of the peak, resembling the T_g endotherm of mechanically amorphized 1,3,5-tri-α-naphthylbenzene in the curve provided in Figure 2A. The DSC scan had yielded the T_g of water of 136 K for heating at 30 K/min.[8−10,68] Consistent T_g values were obtained for other heating rates.[12] A low-density amorph (LDA) of unknown structure, which had been produced by heating pressure-collapsed hexagonal and cubic ices, had also shown a similar T_g endotherm.[16,46,69,70]

Originally, there were two arguments for the speculated T_g of water of ∼165 K:[71] (i) the enthalpy of unannealed HGW apparently continues to decrease at $T > 136$ K, and (ii) the endotherm with onset at 136 K can also arise from the Bjerrum defects diffusion (see refs 49 and 71−73 for details). These arguments have been withdrawn in ref 29, and it has been speculated that the apparent peak of the T_g endotherm observed for HGWs is a sub-T_g peak (which requires molecular diffusion) and the T_g of water is in the 165−180 K range,[29] which cannot be observed because *glassy water crystallizes* too rapidly in the 148−155 K range, much before 165 K is reached. (Note that the Bjerrum defects diffusion mechanism for an endotherm used in ref 71 had been suggested by Fisher and Devlin[72] and was based on their isotopic exchange kinetics data of doped ASW. This mechanism has been reconsidered[73] and the kinetics data reinterpreted in terms of translational diffusion of water molecules.) To determine the merits of this suggestion, we recall the DSC scans of preannealed ASW and HGW obtained in our earlier studies,[8,11,13] as well as the DSC scan of LDA.[69,70] The relevant parts of these scans are shown in Figure 2B. (To avoid confusion, it is to be noted that the DSC scans of ASW and HGW in Figure 5 of ref 29 differ from those in the original figure in the literature.) A comparison of these DSC scans against the sub-T_g peak of $Zr_{55}Cu_{45}$ glass, which is shown by curve 1 in Figure 1C, indicates that features of these scans do not resemble the sub-T_g peak of the $Zr_{55}Cu_{45}$ glass. Even if the ASW and HGW scans are seen to resemble the sub-T_g peak of the $Zr_{55}Cu_{45}$ glass, there are notable characteristic differences. The slope on the right-hand side of the sub-T_g peak in Figure 1C is gentle and has an inflection closer to the peak. In contrast, the corresponding slope of the apparent peak of the T_g endotherm for ASW, HGW, and LDA in Figure 2B is steep, and its inflection is near the minimum of the crystallization exotherm shown in Figure 5 in ref 29. Rather, these endotherms resemble the T_g endotherm of mechanically amorphized 1,3,5-tri-α-naphthylbenzene shown in Figure 1A.

One may argue that crystallization exotherm of HGW and ASW joins up with the relaxational decrease in (dH/dt) of the

sub-T_g peak, and hence, the slope becomes increasingly more negative. But, this would entail that preannealed ASW and HGW have crystallized in the presumed (rigid) glassy state at a temperature far below the speculated T_g of 165 K[71] or 160−180 K,[29] which puts the 136−150 K range in the sub-T_g peak region. It is well-known that (rigid solid) glasses *do not begin to* congruently *crystallize* in a period of a few minutes when kept at a temperature slightly below T_g. Moreover, crystallization kinetics of both preannealed and unannealed states of HGW has been studied by FTIR over the 138−155 K range for H_2O (147−152 K range for D_2O) and over a period of several hours.[74,75] It was found that crystallization to cubic ice[74,75] follows the known kinetics formalism for a viscous liquid. Because crystallization has been observed in the range covering the endotherm from 136−148 K, we conclude that the DSC scan of HGW fulfills the first criteria (of crystallization) for T_g endotherm and not that (no-crystallization) for a sub-T_g peak.

Before using criteria 2, 3, and 4, we note that Kohl et al,[14] have produced HGW by depositing ∼5 μm diameter droplets on a substrate kept at ca. 140 K, a temperature much higher than ca. 77 K used in the earlier preparation of HGW.[8] They cooled the sample from 140 to 77 K and obtained its DSC scan without annealing the sample.[14] As discussed here earlier, the onset of a sub-T_g peak occurs at $T = T_{ann}$ and not at $T < T_{ann}$.[8−28] Accordingly, if the endotherm observed by Kohl et al[14] was to be a sub-T_g peak, its onset temperature would be 140 K. The DSC scan of this *unannealed* HGW measured for a 30 K/min heating rate instead showed an endotherm (see the fifth curve from the top in Figure 1B of ref 14) with an onset temperature of ca. 136 K, consistent with the values obtained in the earlier studies.[8−12] Because this *unannealed* HGW has shown onset of the endotherm at about the same temperature as HGW preannealed at several temperatures near 130 K for different periods,[8−12] criterion 2 for the sub-T_g peak is not fulfilled. Also, the unannealed HGW in ref 14 shows an endothermic peak just like the *annealed* HGW,[8−12] and the height and temperature of the peak did not change when T_{ann} and annealing time was varied in earlier studies.[8−12] Therefore, criterion 3 for the sub-T_g peak is not fulfilled. Because HGW in this study[14] remained a highly viscous liquid at ca. 140 K and its DSC scan showed a slightly positive or even zero slope prior to the onset temperature (unannealed HGW has already shown a negative slope due to structural relaxation[52]), criterion 4 for the sub-T_g peak is not fulfilled. We conclude that the DSC endotherm for HGW fulfills criteria 1−4 for the T_g endotherm and not those for a sub-T_g peak.

7. Glass-Softening and Subsequent Crystallization of Unusually Formed Amorphous Solids

Amorphous solids of unusually high enthalpy are common in nature. For example, water accreted on particles in comets is believed to be amorphous with high enthalpy frozen-in during its formation or high enthalpy pumped-in by the ambient, high-energy ultraviolet, electron, neutron, or α-particle irradiations or both. Also, in technologies of cryopreservation and cryofixation, biological fluids are vitrified by quenching in liquid nitrogen, and in the technologies of production of electronic components, amorphous thin films are produced by vapor deposition. Furthermore, mechanical amorphization of crystals also produces a high-enthalpy amorphous solid.[34−40] Examples of such amorphous solids are metal alloys,[34−38] SiO_2,[39] Se,[40] medicaments such as aspirin[76] and *β-cyclo*-dextrin,[77] and a variety of organic compounds.[41,42] A number of mechanically amorphized solids have been studied by adiabatic calorimetry, differential thermal analysis (DTA), and DSC. These have shown features similar to those of hyperquenched glasses and vapor-deposited amorphous solids.

TABLE 1: The Glass-Softening Temperature, T_g, Measured from the Onset of the Endotherm, the Temperature of Onset of the Crystallization Exotherm, T_{cryst}, and the Ratio, T_{cryst}/T_g, for Several Materials Initially Obtained in the High-Enthalpy State by Vapor Deposition (VD), Hyperquenching of the Liquid (HQL), Normal Cooling of the Liquid (NCL), and Mechanical Amorphization of the Crystals (MAC)[a]

amorphous solids	T_g (K)	T_{cryst} (K)	(T_{cryst}/T_g)
propene (VD) (3, 4, 6)	56	63	1.13
propane (VD) (3, 4)	45.5	48.7	1.07
1-pentene (VD) (3, 4, 78)	71.7	93.8	1.31
1-pentene (NCL) (3, 78)	71.2	99.8	1.40
chloroform (VD) (6)	84	88	1.05
methanol (VD) (7)	103	106	1.03
butyronitrile (VD) (79)	97	107	1.10
butyronitrile (NCL) (79)	97	107	1.10
tri-*o*-methyl-*β-cyclo*-dextrin (NCL) (41)	345	370	1.07
tri-*o*-methyl-*β-cyclo*-dextrin (MAC) (41, 44)	345	350	1.01
tri-*o*-methyl-*β-cyclo*-dextrin−benzoic acid (NCL) (42)	337		
tri-*o*-methyl-*β-cyclo*-dextrin−benzoic acid (MAC) (42)	337	353	1.05
1,3,5-tri-α-naphthylbenzene (NCL) (44)	345		
1,3,5-tri-α-naphthylbenzene (MAC) (44)	345	355	1.03
$Zr_{41.2}Ti_{13.8}Cu_{12.5}Ni_{10}Be_{22.5}$ (NCL) (80)	620	692	1.12
$Zr_{41}Ti_{14}Cu_{12.5}Ni_{10}Be_{22.5}$ (NCL) (17)	626	692	1.10
$Zr_{41}Ti_{14}Cu_{12.5}Ni_8Fe_2Be_{22.5}$ (NCL) (17)	622	675	1.09
$Zr_{41}Ti_{14}Cu_{12.5}Ni_5Fe_5Be_{22.5}$ (NCL) (17)	630	679	1.08
$Fe_{80}B_{20}$ (HQL) (51)	714	721	1.01
$Fe_{40}Ni_{40}B_{20}$ (HQL) (51)	715	724	1.01
$Fe_{40}Ni_{40}P_{14}B_6$ (HQL) (51)	678	687	1.03
$Ni_{75}P_{16}B_6Al_3$(HQL) (50)	690	700	1.04
$Ni_{68.3}Cr_{6.6}Fe_{2.6}Si_{7.8}C_{0.3}B_{14.4}$ (HQL) (15)	514	640	1.24
$Cu_{88.2}Sn_{11.8}$ (HQL) (15)	437	605	1.38
$Cu_{76.1}Sn_{4.8}Ni_6P_{13.1}$ (HQL) (15)	465	490	1.05
$Co_{70}Fe_5Si_{15}B_{10}$ (HQL) (15)	467	600	1.28
$Fe_{41}Ni_{40}B_{19}$ (HQL) (15)	545	735	1.35
$Fe_{75.4}Cr_5C_{11}P_8Si_{0.4}Mn_{0.2}$ (HQL) (15)	605	726	1.20
$Fe_{80}P_{17}Si_{13}$ (HQL) (15)	528	737	1.39
$Ni_{78}Si_{10}B_{12}$ (HQL) (15)	570	747	1.31
$Ni_{77}Fe_{15}Cu_4Mo_4$ (HQL) (15)	467	610	1.31
$Pd_{50}Cu_{34}P_{16}$ (HQL) (81)	589	613	1.05
$Pd_{50}Cu_{35}P_{15}$ (HQL) (81)	585	613	1.05
$Pd_{50}Cu_{27}P_{23}$ (HQL) (81)	565	592	1.05
water (VD) (68)	136	150	1.10
water (HQL) (68)	136	150	1.10
water (pressure-amorphized ice) (68)	129	152	1.18

[a] Reference to the source of data is indicated in parentheses.

As described earlier here, hyperquenched glasses and mechanically amorphized solids crystallize rapidly on heating to T above their T_g range and in some cases at T within the glass-softening range. Their T_g value has been determined from the onset temperature of their endotherm, and T_{cryst} has been determined from the onset temperature of the exotherm. Adiabatic calorimetry, DTA, and DSC methods all have been used for such measurements. To provide their glass-softening and crystallization characteristics, we have collected their T_g and T_{cryst} values from the literature and listed these in Table 1, where refs 78−81 are cited. The ratio T_{cryst}/T_g, which indicates the proximity of the crystallization and glass-softening temperatures, is also listed in Table 1. Its magnitude has been found to decrease when the heating rate is decreased. When this ratio approaches unity, crystallization temperature approaches the glass-softening range. In this regard, we recall conclusion of Takeda et al.,[4] "...the crystallization of the vapor-deposited *n*-alkanes below their hypothetical T_g seems to be paradoxical"

and note similar mentions for CS_2 the T_g of which has not been measured. These liquids have low freezing points, which decrease with decrease in the size of the liquid droplet—a phenomenon known as the Gibbs−Thomson effect. For that reason, more careful and controlled studies may be needed to produce their glassy states and to determine their T_g.

For materials listed in Table 1, the ratio T_{cryst}/T_g is between 1.01 and 1.10 for 22 out of 35 materials for the heating rates used in their studies. The values for tri-*o*-methyl-*β*-*cyclo*-dextrin listed in Table 1 also show that the T_g of its vitrified state is the same as the onset temperature of the endothermic peak of its mechanically amorphized state, which looked like a sub-T_g peak. Tri-*o*-methyl-*β*-*cyclo*-dextrin−benzoic acid adduct and 1,3,5-tri-α-naphthylbenzene show the same features. We stress that were it not known that the endotherm's onset temperature agrees with the independently determined T_g of the glasses listed in Table 1, their apparent peak of the T_g endotherm would have been misidentified as a sub-T_g peak, and the T_g of the materials would have been speculated to be much higher than the real T_g.

8. Concluding Remarks

A variety of glasses made from vapor deposition, hyperquenching, and mechanical deformation crystallize on heating immediately above their T_g endotherm and produce DSC features that roughly resemble a sub-T_g peak. The DSC features of their T_g endotherm can be distinguished from those of a sub-T_g peak by using the following four criteria: (1) An annealed glass may crystallize slowly on keeping at a fixed T in the range of the T_g endotherm or heating through it and crystallize rapidly at T immediately above that range. It *does not* crystallize at a temperature in the sub-T_g peak range. (2) The onset of a T_g endotherm occurs at $T > T_{ann}$. In contrast, the onset of a sub-T_g peak occurs at T equal to T_{ann}, and its height and area vary when T_{ann} and the annealing time are varied. (3) An *unannealed* glass shows a T_g endotherm. It does not show a sub-T_g peak. (4) The slope of the DSC scan of the *unannealed* state of a glass may remain positive, become zero, and even become negative prior to the onset of the T_g endotherm. The corresponding slope of the *preannealed* state always remains positive prior to the onset of the sub-T_g peak.

By using these criteria, we find that the well-known endothermic feature observed for glassy water cannot be regarded as a sub-T_g peak, and it is a T_g endotherm. This removes the basis for the recent suggestion that the T_g of water is in the 160−180 K range. Had these criteria been used earlier, the T_g endotherm of ASW and HGW could not be mistaken for a sub-T_g peak.

It is also to be noted that water deforms like a viscous liquid at 143 K,[82] and its self-diffusion coefficient corresponds to that of a liquid at ∼155 K.[83] These studies have been reviewed earlier.[84] A large number of vitrified or otherwise amorphized solids have shown crystallization onset temperatures of $1.01T_g$ to $1.10T_g$, thereby making their T_g endotherm appear like a sub-T_g peak. The T_g of a material's vitrified state is about the same as that of its (differently) amorphized state.

Because we have mentioned the T_g of a low-density amorph (LDA) here, it is important to note in this context two recent neutron diffraction studies[47,85] of the transformation of HDA to LDA. These have shown that a multiplicity of amorphous states of both HDA and LDA exist and that discrete states of LDA can persist on heating to ca. 140 K. This means that the T_g of LDA would vary according to the state formed when pressure, time, and temperature conditions of its production are varied. In that case, LDA produced by a different set of pressure, transformation time, and temperature conditions would have a T_g different from the T_g of ca. 129 K for LDA produced earlier and characterized[70] by the exotherm of HDA → LDA transformation and not by diffraction methods.

We also mention some further implications of these findings. Hyperquenched glasses resemble the state obtained by configurational freezing of a liquid in computer simulation, because vitrification in both cases occurs at a high temperature at which the viscosity is low and the diffusion coefficient is high. Because the α-relaxation process, of which the kinetic slowing leads to vitrification, is absent from the low-viscosity liquid and this process evolves only after the liquid's viscosity has reached a certain high value, hyperquenching and computer simulation would not produce a structure in which the α-process occurs. Therefore, like hyperquenching, the state produced by the current computer simulations would be distinguished from the state obtained by normal vitrification. Because hyperquenched glasses densify rapidly on annealing at a fixed T, it is expected that the potential energy landscape, which is used for their description, would change in a manner that produces a deeper energy minimum corresponding to the α-relaxation process. How the potential energy surface itself would change as a glass spontaneously densifies isothermally is not known, but experiments have shown a large decrease in both the diffusion coefficient at a fixed T and the population of molecules participating in localized motions.[86] We propose that experimental studies of such high-enthalpy frozen-in glasses may be useful in guiding the computer simulations.

There are both technological and academic advantages in producing and studying the hyperquenched state of liquids, of orientationally disordered crystals, and of proteins. While their technical importance is well-known from the technologies of cryopreservation, microelectronics, and high strength metal-alloys, their academic importance is not known. We mention some of these here: By virtue of their kinetic freezing at a temperature much higher than the crystallization and disorder−order transformation temperatures, hyperquenched states can override these transformations, and when annealed at a suitable temperature, a hyperquenched solid may crystallize or undergo an ordering transformation only very slowly. This slow occurrence would allow study of the intermediate states of the transformation in real time. We also note that even normal cooling has been found to kinetically freeze the disordered state of cubic and hexagonal ices[87,88] and of ice clathrates[89] and thus to hide their orientational ordering transformations. Annealing and further heating of such states have already shown beginning of partial-ordering, which becomes arrested by the development of the strain energy at the two-phase interface leading to a thermoelastic equilibrium.[90] The resulting avalanche-like nature of such transitions in hexagonal ice and ice clathrates has recently been examined.[91] Also, because mechanically amorphized solids behave like hyperquenched glasses, these would be useful for the abovementioned purpose of observing stages of phase transformations. Studies of hyperquenched kinetically frozen states of high fictive temperature of proteins would be particularly valuable in investigating the various stages of protein transitions in real time and then isolating the states at different stages of the transformation. Studies of quenched states of beef proteins,[92] wheat gluten,[93,94] gliadin,[95] and soybean[96] (vegetable proteins) and of chemical reactions approaching an equilibrium[97] have been aimed at understanding such processes.

Acknowledgment. I am grateful to the Natural Sciences and Engineering Research Council of Canada for a general research grant.

References and Notes

(1) Roy, R. *J. Non-Cryst. Solids* **1970**, *3*, 33.
(2) Johari, G. P. *J. Chem. Educ.* **1974**, *51*, 23.
(3) Takeda, K.; Oguni, M.; Suga, H. *Thermochim. Acta* **1990**, *158*, 195.
(4) Takeda, K.; Oguni, M.; Suga, H. *J. Phys. Chem. Solids* **1991**, *52*, 991.
(5) Suga, H.; Oguni, M. In *Chemical Thermodynamics, A Chemistry for 21st Century*; Letcher, T. M., Ed.; Blackwell: London, 2001; Chapter 19, p 227.
(6) Haida, O.; Suga, H.; Seki, S. *Thermochim. Acta* **1972**, *3*, 177.
(7) Sugisaki, M.; Suga, H.; Seki, S. *Bull. Chem. Soc. Jpn*. **1968**, *41*, 2586.
(8) Johari, G. P.; Hallbrucker, A.; Mayer, E. *Nature* **1987**, *330*, 552.
(9) Hallbrucker, A.; Mayer, E.; Johari, G. P. *Philos. Mag. B* **1989**, *60*, 179.
(10) Johari, G. P.; Hallbrucker, A.; Mayer, E. *J. Chem. Phys.* **1990**, *92*, 6742.
(11) Johari, G. P.; Astl, G.; Mayer, E. *J. Chem. Phys*. **1990**, *92*, 809.
(12) Tulk, C. A.; Klug, D. D.; Brandenhorst, R.; Sharp, P.; Ripmeester, J. A. *J. Chem. Phys*. **1998**, *109*, 8478.
(13) Hallbrucker, A.; Mayer, E.; Johari, G. P. *J. Phys. Chem*. **1989**, *93*, 4986.
(14) Kohl, I.; Hallbrucker, A.; Mayer, E. *Phys. Chem. Chem. Phys*. **2000**, *2*, 1579.
(15) Ram, S.; Johari G. P. *Philos. Mag*. *B* **1990**, *61*, 299.
(16) Handa, Y. P.; Klug, D. D. *J. Phys. Chem*. **1988**, *92*, 3323.
(17) Zhuang, Y. X.; Wang, W. H.; Zhang, Y.; Pan, M. X.; Zhao, D. Q. *Appl. Phys. Lett*. **1999**, *75*, 2392.
(18) Drijver, J. W.; Musder, A. L.; Emmens, W. C.; Radelaar, S. In *Proceedings of the IInd International Conference on Rapidly Quenched Metals*; Cantor, B., Ed.; Metal Society: London, 1978; Vol. 2, p 96.
(19) Chen, H. S. In *Proceedings of the 4th International Conference on Rapidly Quenched Metals, Sendai, 1981*; Matsumoto, T.; Suzuki, K. Eds.; The Japan Institute of Metals: Sendai, Japan, 1982; p 495.
(20) Chen, H. S. *J. Appl. Phys.* **1981**, *52*, 1868.
(21) Chen, H. S.; Wang, T. T. *J. Appl. Phys*. **1981**, *52*, 5898.
(22) Chen, H. S.; Kurkjian, C. R. *J. Am. Ceram. Soc*. **1983**, *66*, 613.
(23) Chen, H. S. *J. Non-Cryst. Solids* **1981**, *46*, 289.
(24) Inoue, A.; Matsumoto, T.; Chen, H. S. *J. Mater. Sci.* **1984**, *19*, 3953.
(25) Chen, H. S.; Inoue, A. *J. Non-Cryst. Solids* **1984**, *61 & 62*, 805.
(26) Inoue, A.; Matsumoto, T.; Chen, H. S. *J. Mater. Sci*. **1985**, *20*, 4057.
(27) Chen, H. S.; Inoue, A.; Matsumoto, T. *J. Mater. Sci*. **1985**, *20*, 2417.
(28) Inoue, A.; Matsumoto T.; Chen, H. S. *J. Non-Cryst. Solids* **1986**, *83*, 297.
(29) See "Note Added in Proof" on p 2647 in: Angell, C. A. *Chem. Rev*. **2002**, *102*, 2627. Two arguments had been used for speculating that the T_g of water is 165 K: (i) the observed enthalpy release occurs over a broad temperature range and (ii) the onset of the Bjerrum defects diffusion would produce a T_g endotherm. On pp 2632−2635 of this paper, these arguments have been abandoned and opposite arguments are used to allow self-diffusion necessary for speculating that water's T_g endotherm[8−14] may be a sub-T_g peak.
(30) Suga H.; Seki, S. *Thermochim. Acta* **1986**, *100*, 149.
(31) Mishima, O.; Calvert, L. D.; Whalley, E. *Nature* **1984**, *310*, 393.
(32) Skinner, B. J.; Fahey, J. J. *J. Geophys. Res.* **1963**, *68*, 5595.
(33) Bosio, L.; Johari, G. P.; Teixiera, J. *Phys. Rev. Lett*. **1986**, *56*, 460.
(34) Schwarz, R. B., Johnson, W. L., Eds. *Solid State Amorphizing Transformations*; Journal of the Less−Common Metals, Vol. 140; Elsevier: New York, 1988.
(35) Suzuki, K., Wright, A. C., Eds. *Structure of Non-Crystalline Materials*; Journal of Non-Crystalline Solids, Vol. 150; Elsevier: New York, 1992; Sect. 12.
(36) Hen, Z. *J. Phys.: Condens. Matter* **1993**, *5*, L337
(37) Kanazawa, T.; Oguchi, T.; Ohta, T.; Tokumitsu, K.; Sakurai, Y.; Nanano, S.; Iwashita, T. *Phys. Rev. B* **1993**, *47*, 7732.
(38) Chen, Y.; Bibole, M.; Le Hazif, R.; Martin, G. *Phys. Rev. B* **1993**, *48*, 14.
(39) Wright, A. C.; Bachra, B.; Brunier, T. M.; Sinclair, R. N.; Gladden, L. F.; Portsmouth, R. L. *J. Non-Cryst. Solids* **1992**, *150*, 69.
(40) Chan, S. L.; Gladden, L. F.; Elliott, S. R. *J. Non-Cryst. Solids* **1988**, *106*, 413.
(41) Tsukushi, I.; Yamamuro, O.; Suga, H. *J. Non-Cryst. Solids* **1994**, *175*, 187.
(42) Tsukushi, I.; Yamamuro, O.; Suga, H. *Thermochim. Acta* **1992**, *200*, 71.
(43) Tsukushi, I.; Yamamuro, O.; Suga, H. *J. Therm. Anal*. **1995**, *45*, 905.
(44) Yammauro, O.; Tsukushi, I.; Matsuo, T. *Mol. Cryst. Liq. Cryst.* **1996**, *277*, 205.
(45) Tsukushi, I.; Yamamuro, O.; Ohta, T.; Matsuo, T.; Nakano, H.; Shirota, Y. *J. Phys.: Condens. Matter* **1996**, *8*, 245.
(46) Johari, G. P.; Hallbrucker, A.; Mayer, E. *Science* **1996**, *273*, 90.
(47) Tulk, C. A.; Benmore, C. J.; Urquidi, J.; Klug, D. D.; Neuefeind, J.; Tomberli, B.; Egelstaff, P. A. *Science* **2002**, *297*, 1320.
(48) Oguni, M.; Hikawa, H.; Suga, H. *Thermochim. Acta* **1990**, *158*, 143.
(49) Johari, G. P. *J. Chem. Phys.* **2002**, *116*, 8067.
(50) Coleman, E. *Mater. Sci. Eng.* **1976**, *23*, 161.
(51) Luborsky, F. E. *Mater. Sci. Eng*. **1977**, *28*, 139.
(52) Hallbrucker, A.; Mayer, E. *J. Phys. Chem*. **1987**, *91*, 503.
(53) Hofer, K.; Hallbrucker, A.; Mayer, E.; Johari, G. P. *J. Phys. Chem*. **1989**, *93*, 4674.
(54) Hofer, K.; Astl, G.; Mayer, E.; Johari, G. P. *J. Phys. Chem*. **1991**, *95*, 10777.
(55) Scherer, G. W. *Relaxations in Glass and Composites*; Wiley: New York, 1986.
(56) Hodge, I. M. *J. Non-Cryst. Solids* **1994**, *169*, 211.
(57) Magill, J. H. *J. Chem. Phys*. **1967**, *47*, 2802.
(58) Whitaker, C. M.; McMahon, R. J. *J. Phys. Chem*. **1996**, *100*, 1081.
(59) Sartor, G.; Johari, G. P. *J. Phys. Chem. B* **1999**, *103*, 11036.
(60) Plazek, D.; Magill, J. H. *J. Chem. Phys*. **1968**, *49*, 3678.
(61) Cukierman, M.; Lane, J. W.; Uhlmann, D. R. *J. Chem. Phys*. **1973**, *59*, 3639.
(62) Magill, J. H.; Plazek, D. J. *J. Chem. Phys*. **1967**, *46*, 3757.
(63) Ngai, K. L.; Magill, J. H.; Plazek, D. J. *J. Chem. Phys*. **2000**, *112*, 1887.
(64) Plazek, D. J.; Magill, J. H. *J. Chem. Phys*. **1966**, *45*, 3038.
(65) Hofer, K.; Perez, J.; Johari, G. P. *Philos. Mag. Lett*. **1991**, *64*, 37.
(66) Plazek, D. J.; Magill, J. H.; Echeverria, I.; Chay, I.-C. *J. Chem. Phys*. **1999**, *110*, 10445.
(67) Mayer, E. *J. Appl. Phys*. **1985**, *58*, 663.
(68) Mayer, E. In *Hydrogen Bond Networks*; Bellissent-Funel, M. C., Dore, J. C., Eds.; Kluwer: Dordrecht, Netherlands, 1994; p 355; *J. Mol. Struct*. **1991**, *250*, 403.
(69) Hallbrucker, A.; Mayer, E.; Johari, G. P. *J. Phys. Chem*. **1989**, *93*, 7751.
(70) Johari, G. P.; Hallbrucker, A.; Mayer, E. *J. Phys. Chem.* **1990**, *94*, 1212.
(71) Velikov, V.; Borick, S.; Angell, C. A. *Science* **2001**, *294*, 2335.
(72) Fisher, M.; Devlin, J. P. *J. Phys. Chem*. **1995**, *99*, 11548.
(73) Johari, G. P. *J. Chem. Phys*. **2002**, *117*, 2782.
(74) Hage, W.; Hallbrucker, A.; Mayer, E.; Johari, G. P. *J. Chem. Phys*. **1994**, *100*, 2743.
(75) Hage, W.; Hallbrucker, A.; Mayer, E.; Johari, G. P. *J. Chem. Phys*. **1995**, *103*, 545.
(76) Johari, G. P.; Pyke, D. *Phys. Chem. Chem. Phys*. **2000**, *2*, 5479.
(77) Tsukushi, I.; Yamamuro, O.; Matsuo, T. *Solid State Commun*. **1995**, *94*, 1013.
(78) Takeda, K.; Yamamuro, O.; Suga, H. *J. Phys. Chem*. **1995**, *99*, 1602.
(79) Hikawa, H.; Oguni, M.; Suga, H. *J. Non-Cryst. Solids* **1988**, *101*, 90.
(80) Busch, R.; Kim, Y. J.; Johnson, W. L. *J. Appl. Phys*. **1995**, *77*, 4039.
(81) Schwarz, R. B.; He, Y. In *Properties of Complex Inorganic Solids*; Gonis, A., Meike, A., Turchi, P. E. A., Eds.; Plenum: New York, 1997; p 287.
(82) Johari, G. P. *J. Phys. Chem*. *B* **1998**, *102*, 4711 (ref 21 in this paper should read, *Science*, **1996**, *273*, 90).
(83) Smith, R. S.; Dohnalek, Z.; Kimmel, G. A.; Stevenson, K. P.; Kay, B. D. *Chem. Phys.* **2001**, *258*, 291.
(84) Johari, G. P. *J. Mol. Struct*. **2000**, *520*, 249.
(85) Koza, M. M.; Schober, H.; Fischer, H. E., Hansen, T.; Fujara, F. *J. Phys.: Condens. Matter* **2003**, *15*, 321.
(86) Johari, G. P. *J. Non-Cryst. Solids* **2002**, *307−310*, 387.
(87) Johari, G. P. *J. Chem. Phys.* **1998**, *109*, 9543.
(88) Johari, G. P. *Chem. Phys.* **2000**, *258*, 277.
(89) Suga, H.; Matsuo, T.; Yamamuro, O. *Supramol. Chem.* **1993**, *1*, 221.
(90) Johari, G. P. *Philos. Mag. A* **1999**, *79*, 1479.
(91) Johari, G. P. *Chem. Phys.*, submitted for publication.
(92) Sartor, G.; Johari, G. P. *J. Phys. Chem.* **1996**, *100*, 10450, 6791.
(93) Johari, G. P.; Sartor, G. *J. Chem. Soc., Faraday Trans.* **1996**, *92*, 4521; **1997**, *93*, 2609.
(94) Sartor, G.; Johari, G. P. *J. Phys. Chem.* **1996**, *100*, 19692, 6791.
(95) Ferrari, C.; Johari, G. P. *Int. J. Biol. Macromol.* **1997**, *21*, 231.
(96) Johari, G. P.; Sartor, G. In *Proceedings of the International Symposium on the Properties of Water in Foods*; Reid, D. C., Ed.; Blackie Academic: London, 1998; Chapter V, pp 103−138.
(97) Wasylyshyn, D. A.; Johari, G. P.; Tombari, E.; Salvetti, G. *Chem. Phys.* **1997**, *223*, 313.